

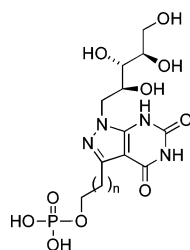
A New Series of 3-Alkyl Phosphate Derivatives of 4,5,6,7-Tetrahydro-1-D-ribityl-1H-pyrazolo[3,4-d]pyrimidinedione as Inhibitors of Lumazine Synthase: Design, Synthesis, and Evaluation

Yanlei Zhang,[†] Guangyi Jin,[†] Boris Illarionov,[‡] Adelbert Bacher,[‡] Markus Fischer,[§] and Mark Cushman^{*,†}

Department of Medicinal Chemistry and Molecular Pharmacology, School of Pharmacy and Pharmaceutical Sciences, and the Purdue Cancer Center, Purdue University, West Lafayette, Indiana 47907, Lehrstuhl für Organische Chemie und Biochemie, Technische Universität München, Lichtenbergstr. 4, D-85747 Garching, Germany, and Institut für Lebensmittelchemie, Abteilung Lebensmittelchemie, Universität Hamburg, D-20146 Hamburg, Germany

cushman@pharmacy.purdue.edu

Received May 18, 2007



Inhibition Constants vs *Mycobacterium tuberculosis* Lumazine Synthase

n	K_i	mechanism
2	15 ± 4 nM	competitive
3	30 ± 3 nM	competitive
4	40 ± 3 nM	competitive

Lumazine synthase catalyzes the penultimate step in the biosynthesis of riboflavin. A homologous series of three pyrazolopyrimidine analogues of a hypothetical intermediate in the lumazine synthase-catalyzed reaction were synthesized and evaluated as lumazine synthase inhibitors. The key steps of the synthesis were C-5 deprotonation of 4-chloro-2,6-dimethoxypyrimidine, acylation of the resulting anion, and conversion of the product to a pyrazolopyrimidine with hydrazine. Alkylation of the pyrazolopyrimidine with a substituted ribityl iodide and deprotection of the ribityl chain afforded the final set of three products. All three compounds were extremely potent inhibitors of the lumazine synthases of *Mycobacterium tuberculosis*, *Magnaporthe grisea*, *Candida albicans*, and *Schizosaccharomyces pombe* lumazine synthase, with inhibition constants in the low nanomolar to subnanomolar range. Molecular modeling of one of the homologues bound to *Mycobacterium tuberculosis* lumazine synthase suggests that both the hypothetical intermediate in the lumazine synthase-catalyzed reaction pathway and the metabolically stable analogues bind similarly.

Introduction

Riboflavin (vitamin B₂) plays an essential role in metabolism. Animals, including humans, obtain it from their diet, while a variety of pathogenic Gram-negative Enterobacteria and *Candida*- and *Saccharomyces*-type yeasts are dependent on endogenous biosynthesis because they do not have an efficient uptake system.^{1–4} The riboflavin biosynthesis gene *ribB* has recently

been shown to play an essential role in different *Salmonella* disease models.^{5,6} Since animals lack the riboflavin biosynthetic pathway, inhibitors of the pathway should therefore be selectively toxic to the pathogen and not the host. The resistance of bacteria to antibiotics is increasing at a sobering rate, and it is therefore imperative that medicinal chemists develop new types of antibiotics. Riboflavin synthase and lumazine synthase, the last two enzymes in the riboflavin biosynthetic pathway, are promising targets for the development of new antibiotics.

[†] Purdue University.

[‡] Technische Universität München.

[§] Universität Hamburg.

(1) Wang, A. *I Chuan Hsueh Pao* **1992**, *19*, 362–368.

(2) Oltmanns, O.; Lingens, F. Z. *Naturforsch.* **1967**, *22b*, 751–754.

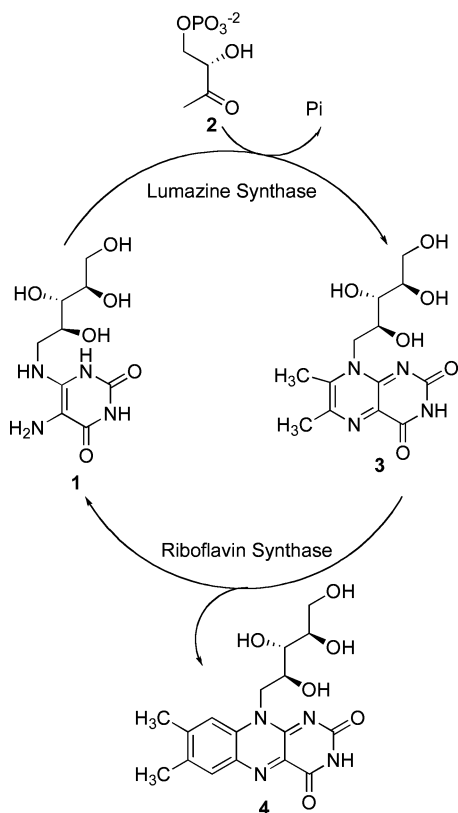
(3) Logvinenko, E. M.; Shavlovsky, G. M. *Mikrobiologiya* **1967**, *41*, 978–979.

(4) Neuberger, G.; Bacher, A. *Biochem. Biophys. Res. Commun.* **1985**, *127*, 175–181.

(5) Rollenhagen, C.; Bumann, D. *Infect. Immunol.* **2006**, *74*, 1649–1660.

(6) Becker, D.; Selbach, M.; Rollenhagen, C.; Ballmaier, M.; Meyer, T. F.; Mann, M.; Bumann, D. *Nature* **2006**, *440*, 303–307.

SCHEME 1

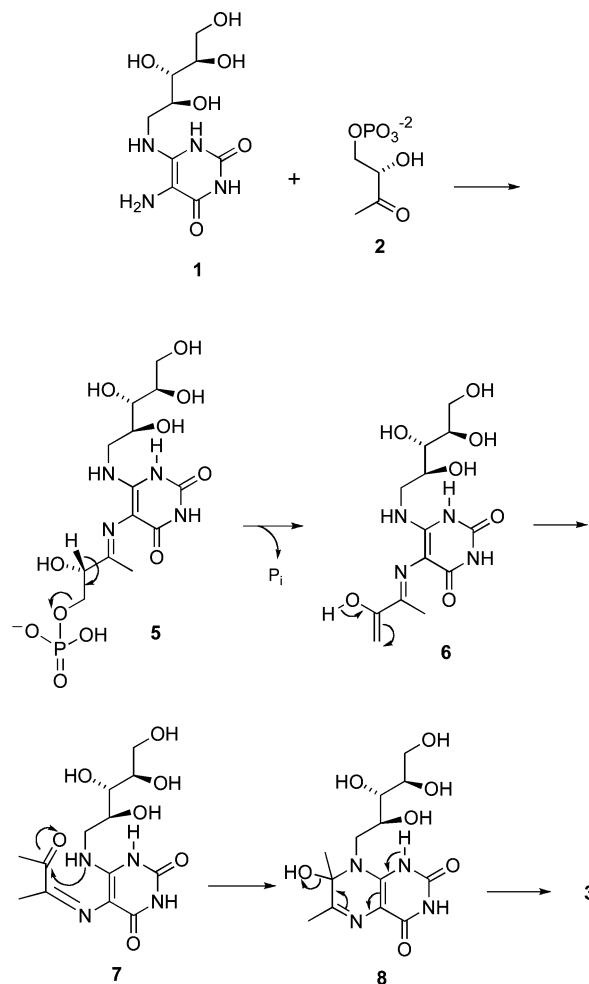


Lumazine synthase catalyzes the condensation of 5-amino-6-D-ribylamino-2,4(1H,3H)-pyrimidinedione (**1**) with 3,4-dihydroxybutanone 4-phosphate (**2**) to afford 6,7-dimethyl-8-D-ribyllumazine (**3**).^{7,8} Riboflavin synthase catalyzes a mechanistically unusual dismutation of two molecules of **3** to form one molecule of riboflavin (**4**) and one molecule of the lumazine synthase substrate **1** (Scheme 1).^{9–13}

The details of the reaction catalyzed by lumazine synthase have not been completely elucidated. The currently proposed mechanism outlined in Scheme 2 involves the condensation of the primary amino group of the substituted pyrimidinedione **1** with the ketone **2** to give Schiff base **5**, elimination of phosphate to yield the enol **6**, tautomerization of the enol **6** to the ketone **7**, ring closure, and dehydration of the covalent hydrate **8** to provide the product **3**.¹⁴ Although the mechanism listed in Scheme 2 is certainly very reasonable, the details of the pathway, such as the timing of phosphate elimination relative to the conformational reorganization of the side chain to allow cyclization, remain unknown.¹⁴

The purinetrione **9** is a moderate inhibitor of *Bacillus subtilis* lumazine synthase. When tested in the presence of a fixed

SCHEME 2



concentration of substrate **1** and variable concentration of substrate **2** in phosphate buffer, the inhibitor dissociation constant K_i is 46 μM and the K_{is} is 250 μM .¹⁵ The installation of a C-4 or C-5 phosphate side chain resulted in **11** and **12**, both of which proved to be less potent than purinetrione **9** on *Bacillus subtilis* lumazine synthase in phosphate buffer. When tested in the presence of variable concentrations of substrate **2** in phosphate buffer, **11** displayed a K_{is} of 852 μM and **12** displayed a K_i of 852 μM and a K_{is} of 817 μM .¹⁶ In contrast, when they were tested on *Mycobacterium tuberculosis* lumazine synthase in Tris buffer, they proved to be very potent inhibitors. The phosphate **11** displayed a K_i of 4.1 nM, and **12** displayed a K_i of 4.7 nM.¹⁶ By comparing with **9** ($K_i = 9.1 \mu\text{M}$) in Tris buffer,¹⁶ the potent contribution of the alkylphosphate side chain toward inhibition of *Mycobacterium tuberculosis* lumazine synthase can be discerned.

The study of purinetrione **9** and its alkylphosphonate derivatives suggests that another series of compounds, the pyrazolopyrimidinediones **13**, **14**, and **15**, could be effective inhibitors of *Mycobacterium tuberculosis* lumazine synthase. The prior study of alkylphosphonate derivatives of purinetrione **9** showed that the C-4 derivative **11** is more potent than the others, which

(7) Neuberger, G.; Bacher, A. *Biochem. Biophys. Res. Commun.* **1986**, *139*, 1111–1116.

(8) Kis, K.; Volk, R.; Bacher, A. *Biochemistry* **1995**, *34*, 2883–2892.

(9) Bacher, A.; Eberhardt, S.; Richter, G. In *Escherichia coli and Salmonella: Cellular and Molecular Biology*, 2nd ed.; Neidhardt, F. C., Ed.; ASM Press: Washington, D.C., 1996; pp 657–664.

(10) Gerhardt, S.; Schott, A.-K.; Kairies, N.; Cushman, M.; Illarionov, B.; Eisenreich, W.; Bacher, A.; Huber, R.; Steinbacher, S.; Fischer, M. *Structure* **2002**, *10*, 1371–1381.

(11) Illarionov, B.; Eisenreich, W.; Bacher, A. *Proc. Natl. Acad. Sci. U.S.A.* **2001**, *98*, 7224–7229.

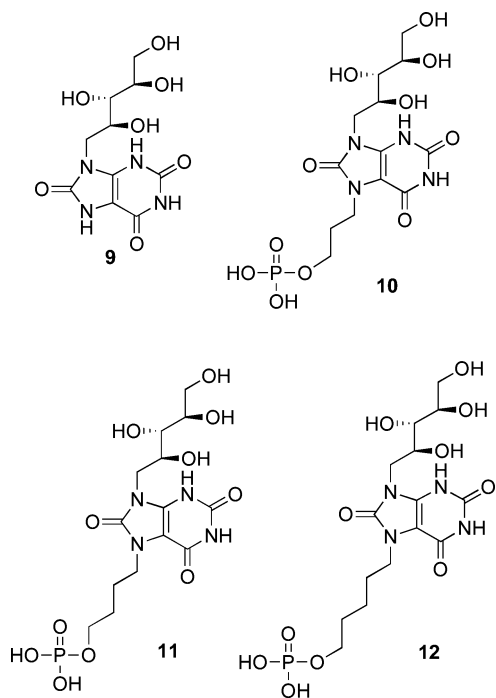
(12) Illarionov, B.; Kemter, K.; Eberhardt, S.; Richter, G.; Cushman, M.; Bacher, A. *J. Biol. Chem.* **2001**, *276*, 11524–11530.

(13) Plaut, G. W. E.; Harvey, R. A. *Methods Enzymol.* **1971**, *18B*, 515–538.

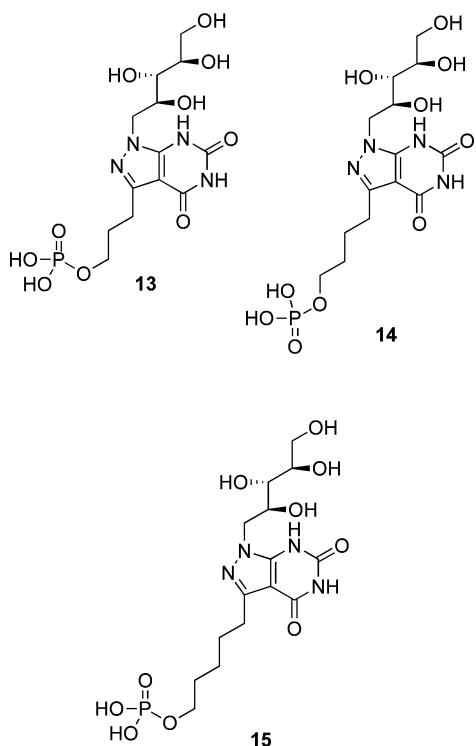
(14) Volk, R.; Bacher, A. *J. Am. Chem. Soc.* **1988**, *110*, 3651–3653.

(15) Cushman, M.; Yang, D.; Kis, K.; Bacher, A. *J. Org. Chem.* **2001**, *66*, 8320–8327.

(16) Cushman, M.; Sambaiah, T.; Jin, G.; Illarionov, B.; Fischer, M.; Bacher, A. *J. Org. Chem.* **2004**, *69*, 601–612.



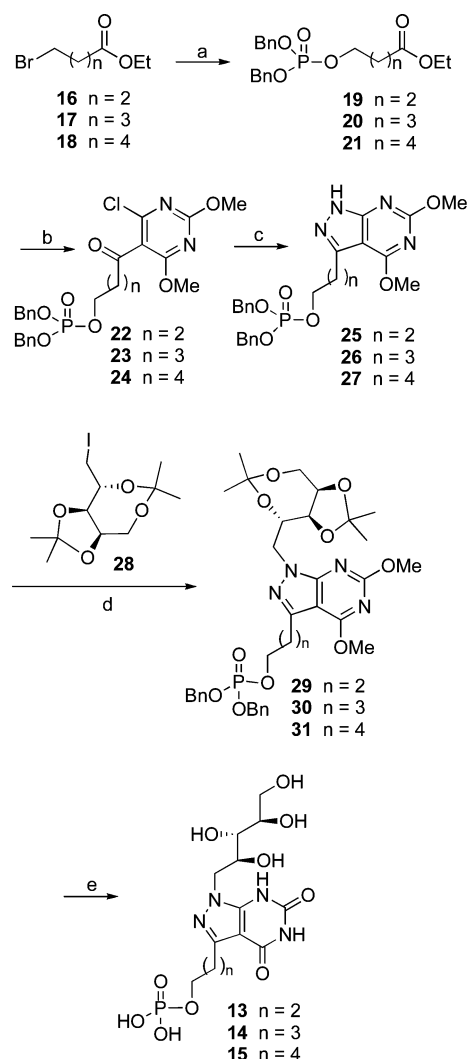
indicates that the C-4 derivative **14** should be the best inhibitor in this new series of compounds.¹⁶ Crystallography has previously shown that the C-6 carbonyl of the purinetriones **9–12** hydrogen bonds with the side chain amino group of Lys138 of lumazine synthase.¹⁷ The hypothesis motivating the present study was that the N-2 nitrogen of the pyrazolo[3,4-*b*]pyrimidine system in the target compounds **13–15** would also hydrogen bond to Lys138 and thus stabilize their complexes with the enzyme.



Results and Discussion

On the basis of the previous study of **9–12**, 3-, 4- and 5-carbon linker chains were chosen for the new pyrazolopyri-

SCHEME 3^a



^a Reagents and conditions: (a) AgOPO(OBn)₂, toluene, reflux (24 h); (b) 4-chloro-2,6-dimethoxypyrimidine, *n*-BuLi, THF, -78°C (20 min), -40°C (1 h); (c) hydrazine, methanol, reflux (18 h); (d) K₂CO₃, DMF, 72 h; (e) concd HCl, MeOH, reflux, 5 h.

midinedione series of inhibitors. The syntheses of the ribityl pyrazolopyrimidinediones **13–15** are outlined in Scheme 3. The alkyl phosphate side chains were synthesized and installed on the commercially available 4-chloro-2,6-dimethoxypyrimidine. Nucleophilic displacement reactions on the three commercially available starting materials **16**, **17**, and **18** with silver dibenzylphosphate resulted in the phosphates **19**, **20**, and **21** having chain lengths of three, four, and five carbons. Commercially available 4-chloro-2,6-dimethoxypyrimidine was deprotonated with *n*-butyllithium at low temperature to afford an anion that reacted with the three ethyl esters **19**, **20**, and **21** to provide intermediates **22**, **23**, and **24**. These reactions of **19**, **20**, and **21** were performed at different temperatures. The temperature must be lower for lower homologue **19**, otherwise, the desired reaction did not occur. Reaction of intermediates **22**, **23**, and **24** with hydrazine provided the dimethoxy pyrazolopyrimidines bearing chains of different lengths. A fully protected acyclic ribose

(17) Morgunova, K.; Meining, W.; Illarionov, B.; Haase, I.; Jin, G.; Bacher, A.; Cushman, M.; Fischer, M.; Ladenstein, R. *Biochemistry* **2005**, *44*, 2746–2758.

TABLE 1. Inhibition Constants versus Lumazine Synthases from *M. tuberculosis*, *M. grisea*, *C. albicans*, and *S. pombe*

compd	parameter	<i>M. tuberculosis</i> ^e	<i>M. grisea</i> ^f	<i>C. albicans</i> ^g	<i>S. pombe</i> ^h	
					phosphate buffer	Tris buffer
13	K_s^a (μM)	55 \pm 8	14.4 \pm 1.1	3.2 \pm 0.3	0.61 \pm 0.08	2.4 \pm 0.2
	K_{cat}^b (min^{-1})	0.16 \pm 0.01	2.69 \pm 0.07	7.2 \pm 0.2	0.90 \pm 0.03	0.71 \pm 0.01
	K_i^c (μM)	0.015 \pm 0.004	0.0020 \pm 0.0007	0.0014 \pm 0.0003	0.021 \pm 0.004	0.00089 \pm 0.00045
	K_{is}^d (μM)					
	mechanism	competitive	competitive	competitive	competitive	competitive
14	K_s (μM)	73 \pm 8	22.6 \pm 2.7	3.2 \pm 0.3	0.73 \pm 0.06	2.4 \pm 0.2
	K_{cat} (min^{-1})	0.29 \pm 0.02	3.6 \pm 0.2	7.2 \pm 0.2	0.95 \pm 0.02	0.70 \pm 0.01
	K_i (μM)	0.030 \pm 0.003	0.00080 \pm 0.00058	0.0009 \pm 0.0003	0.026 \pm 0.003	0.0005 \pm 0.0002
	K_{is} (μM)					
	mechanism	competitive	competitive	competitive	competitive	competitive
15	K_s (μM)	30 \pm 3	14.4 \pm 1.1	3.2 \pm 0.3	1.0 \pm 0.1	2.4 \pm 0.2
	K_{cat} (min^{-1})	0.18 \pm 0.01	2.68 \pm 0.07	7.2 \pm 0.2	0.90 \pm 0.04	0.70 \pm 0.01
	K_i (μM)	0.040 \pm 0.003	0.018 \pm 0.006	0.0037 \pm 0.0005	0.12 \pm 0.03	0.020 \pm 0.002
	K_{is} (μM)		0.101 \pm 0.039		0.32 \pm 0.09	
	mechanism	competitive	mixed	competitive	partial	competitive
11	K_s (μM)	63 \pm 6		5.2 \pm 0.4	3.6 \pm 0.3	2.5 \pm 0.1
	K_{cat} (min^{-1})	1.4 \pm 0.1		7.6 \pm 0.2	2.1 \pm 0.1	1.31 \pm 0.05
	K_i (μM)	0.0041 \pm 0.0023		0.0013 \pm 0.0002	0.008 \pm 0.001	0.0040 \pm 0.0006
	K_{is} (μM)					
	mechanism	competitive		competitive	competitive	competitive
12	K_s (μM)	63 \pm 5		4.0 \pm 0.3	4.7 \pm 0.5	2.5 \pm 0.2
	K_{cat} (min^{-1})	1.40 \pm 0.04		6.9 \pm 0.2	2.3 \pm 0.1	1.3 \pm 0.1
	K_i (μM)	0.0047 \pm 0.0019		0.0077 \pm 0.0013	0.12 \pm 0.02	0.044 \pm 0.011
	K_{is} (μM)					0.36 \pm 0.13
	mechanism	competitive		competitive	competitive	mixed

^a K_s is the substrate dissociation constant for the equilibrium $\text{E} + \text{S} \rightleftharpoons \text{ES}$. ^b K_{cat} is the rate constant for the process $\text{ES} \rightarrow \text{E} + \text{P}$. ^c K_i is the inhibitor dissociation constant for the process $\text{E} + \text{I} \rightleftharpoons \text{EI}$. ^d K_{is} is the inhibitor dissociation constant for the process $\text{ES} + \text{I} \rightleftharpoons \text{ESI}$. ^e Recombinant lumazine synthase from *M. tuberculosis*, assay performed in Tris hydrochloride buffer. ^f Recombinant lumazine synthase from *M. grisea*, assay performed in Tris hydrochloride buffer. ^g Recombinant lumazine synthase from *C. albicans*, assay performed in Tris hydrochloride buffer. ^h Recombinant lumazine synthase from *S. pombe*.

derivative **28** was prepared as described in the literature.¹⁸ The ribityl iodide **28** reacted with **25**, **26**, and **27** to provide the fully protected products **29**, **30**, and **31**. The protecting groups were removed with HCl in methanol at reflux to produce the final products **13**, **14**, and **15**.

The pyrazolopyrimidinedione phosphates **13**, **14**, and **15** were tested as inhibitors of recombinant *M. tuberculosis* lumazine synthase, recombinant *M. grisea* lumazine synthase, recombinant *C. albicans* lumazine synthase, recombinant *S. pombe* lumazine synthase, recombinant *B. subtilis* lumazine synthase β_{60} capsids, recombinant *E. coli* riboflavin synthase, and recombinant *M. tuberculosis* riboflavin synthase. Representative Lineweaver–Burk plots for inhibition of *B. subtilis* lumazine synthase, *C. albicans* lumazine synthase, *M. grisea* lumazine synthase, and *S. pombe* lumazine synthase by inhibitor **14** are presented in Figure S33 (Supporting Information). The inhibition constants and inhibition mechanisms for **13**, **14**, and **15** are listed in Tables 1 and 2. The data for the purinetriene phosphates **11** and **12** are also listed in Tables 1 and 2 for comparison.¹⁶

Comparative analysis of the kinetic data shows that imidazole ring replacement in purinetrienes with a pyrazole ring leads to substantial changes in binding affinity. The most striking effects were observed in tests versus riboflavin synthases of *E. coli* and *M. tuberculosis*: pyrazolopyrimidinediones **13**, **14**, and **15** are essentially incapable of binding to either enzyme, whereas purinetrienes **11** and **12** show inhibition activity in the 2–330 μM range (Table 2).

With respect to the tests versus pentameric lumazine synthase of the pathogenic mycobacterium *M. tuberculosis*, pyrazolopy-

rimidinediones **14** and **15** are approximately 8 times less powerful inhibitors than the corresponding purinetrienes **11** and **12** (Table 1). On the other hand, in tests versus pentameric lumazine synthase of the pathogenic yeast *C. albicans*, the difference in inhibitory potency of these two classes is only about a factor of 2. Very high inhibitory potencies were determined for pyrazolopyrimidinedione **14** versus the pentameric lumazine synthase of fission yeast *S. pombe* (0.5 nM).

Crystallographic studies have previously shown that inorganic phosphate, as well as organic phosphate or phosphonate groups that are part of the structures of substrate **2** analogues, can occupy the binding site for **2** in several lumazine synthases and should act as competitive inhibitors of lumazine synthases.^{17,19,20} For this reason, the influence of inorganic phosphate (100 mM) on the inhibitory potencies of compounds **11**–**15** has been determined for both the homopentameric lumazine synthase of *S. pombe* (Table 1) and the icosahedral (60-mer) lumazine synthase of *B. subtilis* (Table 2). Indeed, inorganic phosphate reduces the inhibitory potencies of all compounds tested versus the *S. pombe* enzyme. Particularly, the difference in the inhibitory potency of pyrazolopyrimidinedione compounds reaches a factor of 50 with **14**, whereas the maximum difference for purinetriene compounds reaches a factor of 3 for **12**. A similar tendency is observed for purinetriene compounds tested versus *B. subtilis* lumazine synthase (variable concentration of **1**). For example, compound **11** reveals a K_i value of 12 μM in Tris hydrochloride and 168 μM in phosphate buffer. In contrast

(19) Ladenstein, R.; Ritsert, K.; Richter, G.; Bacher, A. *Eur. J. Biochem.* **1994**, *223*, 1007–1017.

(20) Meining, W.; Mörtl, S.; Fischer, M.; Cushman, M.; Bacher, A.; Ladenstein, R. *J. Mol. Biol.* **2000**, *299*, 181–197.

(18) Aslani-Shotorbani, G.; Buchanan, J. G.; Edgar, A. R.; Shahidi, P. *K. Carbohydr. Res.* **1985**, *136*, 37–52.

TABLE 2. Inhibition Constants versus *B. subtilis* Lumazine Synthase and Riboflavin Synthases from *E. coli* and *M. tuberculosis*

compd	parameter	<i>B. subtilis</i> ^e lumazine synthase			riboflavin synthases	
		phosphate buffer		Tris buffer	<i>E. coli</i> ^h	<i>M. tuberculosis</i> ⁱ
		variable 1 concn ^f	variable 2 concn ^g	variable 1 concn ^f		
13	K_s^a (μM)	6.2 \pm 0.6	3.8 \pm 0.6	7.6 \pm 0.6	2.6 \pm 0.2	7.7 \pm 1.1
	K_{cat}^b (min^{-1})	1.30 \pm 0.05	0.76 \pm 0.03	3.6 \pm 0.1	3.4 \pm 0.1	0.84 \pm 0.05
	K_i^c (μM)	9.9 \pm 2.3	8.2 \pm 0.9	12 \pm 4		
	K_{is}^d (μM)	72 \pm 30		49 \pm 23	> 1000	> 1000
	mechanism	mixed	competitive	mixed	uncompetitive	uncompetitive
14	K_s (μM)	5.5 \pm 0.5	76 \pm 6	5.5 \pm 0.7	2.6 \pm 0.8	4.6 \pm 0.04
	K_{cat} (min^{-1})	1.4 \pm 0.1	1.39 \pm 0.04	3.1 \pm 0.1	3.5 \pm 0.2	0.76 \pm 0.02
	K_i (μM)	58 \pm 17	98 \pm 19	148 \pm 62		
	K_{is} (μM)	113 \pm 30	335 \pm 94	391 \pm 132	> 1000	> 1000
	mechanism	mixed	mixed	mixed	uncompetitive	uncompetitive
15	K_s (μM)	5.5 \pm 0.5	77 \pm 9	8.0 \pm 0.5	2.5 \pm 0.3	6.6 \pm 0.7
	K_{cat} (min^{-1})	1.42 \pm 0.04	1.40 \pm 0.06	3.2 \pm 0.1	3.2 \pm 0.1	0.63 \pm 0.0
	K_i (μM)	79 \pm 17	181 \pm 68	57 \pm 3		
	K_{is} (μM)	118 \pm 18	297 \pm 98		> 1000	> 1000
	mechanism	mixed	mixed	competitive	uncompetitive	uncompetitive
11	K_s (μM)	3.2 \pm 0.4	26 \pm 2	6.5 \pm 0.7	2.1 \pm 0.2	6.9 \pm 0.7
	K_{cat} (min^{-1})	3.1 \pm 0.1	5.4 \pm 0.1	2.1 \pm 0.1	16.7 \pm 0.4	1.10 \pm 0.03
	K_i (μM)	168 \pm 26		12 \pm 1	332 \pm 83	10.3 \pm 0.9
	K_{is} (μM)		852 \pm 103			
	mechanism	competitive	uncompetitive	competitive	competitive	competitive
12	K_s (μM)	3.8 \pm 0.4	40 \pm 4	7.1 \pm 0.7	2.0 \pm 0.2	4.9 \pm 0.7
	K_{cat} (min^{-1})	3.1 \pm 0.1	3.7 \pm 0.1	2.4 \pm 0.1	16.7 \pm 0.4	1.01 \pm 0.03
	K_i (μM)	271 \pm 85	852 \pm 388	11 \pm 2	2.4 \pm 0.2	1.6 \pm 0.2
	K_{is} (μM)	653 \pm 163	817 \pm 212	55 \pm 20		
	mechanism	mixed	mixed	partial	competitive	competitive

^a K_s is the substrate dissociation constant for the equilibrium $\text{E} + \text{S} \rightleftharpoons \text{ES}$. ^b K_{cat} is the rate constant for the process $\text{ES} \rightarrow \text{E} + \text{P}$. ^c K_i is the inhibitor dissociation constant for the process $\text{E} + \text{I} \rightleftharpoons \text{EI}$. ^d K_{is} is the inhibitor dissociation constant for the process $\text{ES} + \text{I} \rightleftharpoons \text{ESI}$. ^e Recombinant β_{60} capsids from *B. subtilis*. ^f The concentration of the dihydroxybutanone phosphate substrate **2** was held constant during the assay, while the concentration of the pyrimidinedione substrate **1** was varied. ^g The concentration of the pyrimidinedione substrate **1** was held constant during the assay, while the concentration of the dihydroxybutanone phosphate **2** was varied. ^h Recombinant riboflavin synthase from *E. coli*. ⁱ Recombinant riboflavin synthase from *M. tuberculosis*.

to this observation, the pyrazolopyrimidinedione compounds do not show the regularities observed for purinetrione inhibitors. The maximal difference in K_i values reaches a factor of 3 for compound **14** (58 and 148 μM in the presence or absence of 100 mM phosphate in the assay buffer, respectively). A plausible explanation for this effect would be that the contribution of the alkyl phosphate moiety to the inhibitory potencies versus 60-mer *B. subtilis* lumazine synthase is much greater in the case of pyrazolopyrimidinediones than purinetrione compounds. Indeed, in experiments with variable concentrations of dihydroxybutanone phosphate **2**, the K_i values for pyrazolopyrimidinediones vary from 8.2 to 181 μM (**13** and **15**, respectively, Table 2), whereas the inhibitory potencies of the purinetriones **11** and **12** were above 800 μM .

The effect of the linker chain length connecting the phosphate to the heterocyclic system was not great, varying from enzyme to enzyme used in kinetic assays. With *M. tuberculosis* lumazine synthase, the shortest linker chain is the best, but with *M. grisea*, *C. albicans*, and *S. pombe* (in Tris buffer), the medium chain length is the best. With *B. subtilis* lumazine synthase, the shortest chain length is the best, and the medium chain length (C-4) is better than the longer one (C-5) in phosphate buffer, but worse in Tris buffer.

A crystal structure is available of the complex formed between the substrate analogue **11** and *M. tuberculosis* lumazine synthase. The crystal structure of the lower homologue **10** bound to *M. tuberculosis* lumazine synthase has also been determined.¹⁷ These structures allow the rational docking and energy minimization of additional lumazine synthase inhibitors. In the

present case, a hypothetical model was constructed of the binding of the lumazine synthase inhibitor **14** to *M. tuberculosis* lumazine synthase (Figure 1). This model was produced by overlapping the structure of **14** with that of **11** in one of the five equivalent active sites of *M. tuberculosis* lumazine synthase. The structure of **11** was then removed and the energy of the complex minimized using the MMFF94s force field. The resulting Figure 1 was constructed by displaying the amino acid residues calculated to be involved in hydrogen bonding of the protein with ligand **14**, using a maximum distance of 3.5 Å between the donor and acceptor atoms to be considered a hydrogen bond. The calculated structure shows the pyrazolopyrimidinedione ring of the ligand **14** stacked with the indole ring of Trp27. The phosphate of the ligand is extensively hydrogen bonded with the one water molecule, the side chain nitrogens of Arg128, as well as the backbone nitrogens of Gln86 and Thr87 and the side-chain hydroxyl of Thr87. The ribityl hydroxyl groups are hydrogen bonded to the backbone nitrogen and oxygen of Asn114, the side-chain oxygens of Glu61, and the backbone nitrogen of Ile60. The pyrazolopyrimidinedione ring of the ligand is hydrogen bonded to the backbone nitrogen of Ala59, the backbone nitrogen of Ile83, backbone oxygen of Val81, and the side-chain nitrogen of Lys138. These contacts are summarized in Figure 2. It should be noted that the contacts are either similar or identical to those seen in the crystal structure of **11** bound to *M. tuberculosis* lumazine synthase (Figure 3). In general, the medium linker chain length connecting the phosphate to the heterocyclic system afforded the most potent inhibitors. This may reflect the fact that the length of the chain

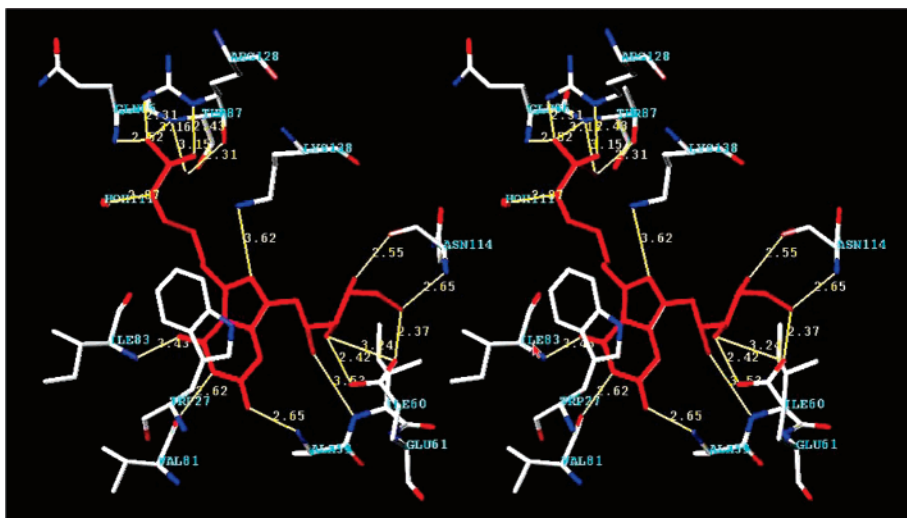


FIGURE 1. Hypothetical model for the binding of compound **14** to *M. tuberculosis* lumazine synthase. The figure is programmed for walled viewing.

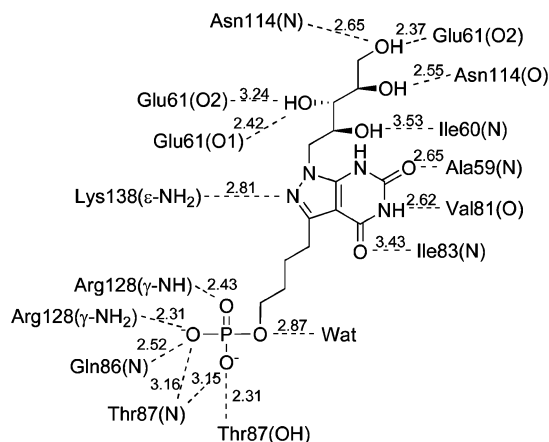


FIGURE 2. Hydrogen bonds and distance in the calculated model of the inhibitor **14** bound in the active site of *M. tuberculosis* lumazine synthase.

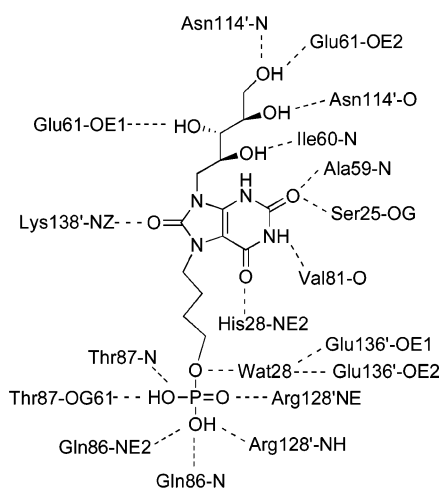


FIGURE 3. The interactions between the *M. tuberculosis* lumazine synthase and the ligand **11** in the crystal structure of the complex.¹⁷

connecting the phosphate to the pyrimidinedione in the hypothetical intermediate **5** is also four atoms in length.

In summary, several very potent inhibitors of the lumazine synthases of a number of important human pathogens, including

M. tuberculosis and *C. albicans*, have been synthesized. These compounds can be considered as bisubstrate analogue inhibitors since they contain the elements of the structures of both substrates **1** and **2** and likely occupy the binding sites of both substrates. They are also metabolically stable hypothetical intermediate analogues that bind similarly to the proposed intermediate **5**. It can be anticipated that these new inhibitors will contribute to the series of metabolically stable analogues of the hypothetical intermediates in the lumazine synthase reaction pathway that have continued to unravel the mechanism of the reactions catalyzed by lumazine synthase and riboflavin synthase.^{10,16,17,20–29}

Experimental Section

3-[4,6-Dioxo-4,5,6,7-tetrahydro-1-D-ribityl-1H-pyrazolo[3,4-d]pyrimidin-3-yl]propyl 1-Phosphate (13). Compound **29** (85 mg, 0.119 mmol) was dissolved in concentrated HCl (1.24 mL) and methanol (1.86 mL). The mixture was heated at reflux for 5 h. The solvent was removed in vacuo to afford the crude product, which was dissolved in water and freeze-dried to yield the product **13** (53 mg, 100%) as an amorphous white solid: ¹H NMR (300 MHz, D₂O) δ 4.06–3.38 (m, 9H), 2.61–2.56 (t, *J* = 7.5 Hz, 2H), 1.82–1.76 (p, *J* = 7 Hz, 2H); ¹³C NMR (75 MHz, D₂O) δ 160.7,

(21) Goetz, J. M.; Poliks, B.; Studelska, D. R.; Fischer, M.; Kugelbrey, K.; Bacher, A.; Cushman, M.; Schaefer, J. *J. Am. Chem. Soc.* **1999**, *121*, 7500–7508.

(22) Scheuring, J.; Kugelbrey, K.; Weinkauff, S.; Cushman, M.; Bacher, A.; Fischer, M. *J. Org. Chem.* **2001**, *66*, 3811–3819.

(23) Mehta, A. K.; Studelska, D. R.; Fischer, M.; Giessauf, A.; Kemter, K.; Bacher, A.; Cushman, M.; Schaefer, J. *J. Org. Chem.* **2002**, *67*, 2087–2092.

(24) Gerhardt, S.; Haase, I.; Steinbacher, S.; Kaiser, J. T.; Cushman, M.; Bacher, A.; Huber, R.; Fischer, M. *J. Mol. Biol.* **2002**, *318*, 1317–1329.

(25) Cushman, M.; Yang, D.; Mihalic, J. T.; Chen, J.; Gerhardt, S.; Huber, R.; Fischer, M.; Kis, K.; Bacher, A. *J. Org. Chem.* **2002**, *67*, 6871–6877.

(26) Zhang, X.; Meining, W.; Cushman, M.; Haase, I.; Fischer, M.; Bacher, A.; Ladenstein, R. *J. Mol. Biol.* **2003**, *328*, 167–182.

(27) Cushman, M.; Jin, G.; Illarionov, B.; Fischer, M.; Ladenstein, R.; Bacher, A. *J. Org. Chem.* **2005**, *70*, 8162–8170.

(28) Ramsperger, A.; Augustin, M.; Schott, A. K.; Gerhardt, S.; Krojer, T.; Eisenreich, W.; Illarionov, B.; Cushman, M.; Bacher, A.; Huber, R.; Fischer, M. *J. Biol. Chem.* **2006**, *281*, 1224–1232.

(29) Morgunova, E.; Illarionov, B.; Sambaiah, T.; Haase, I.; Bacher, A.; Cushman, M.; Fischer, M.; Ladenstein, R. *FEBS J.* **2006**, *273*, 4790–4804.

152.6, 151.5, 146.2, 97.7, 72.8, 72.2, 70.4, 66.3 ($^2J_{PC} = 5.7$ Hz), 62.7, 50.7, 28.6, 23.6; ESIMS m/z 429/430/431 ($C_{13}H_{17}D_4N_4O_{10}PH^+/C_{13}H_{16}D_5N_4O_{10}PH^+/C_{13}H_{15}D_6N_4O_{10}PH^+$). Anal. Calcd for $C_{13}H_{21}N_4O_{10}P \cdot H_2O$: C, 35.30; H, 5.24; N, 12.67. Found: C, 35.40; H, 5.22; N, 12.51.

4-[4,6-Dioxo-4,5,6,7-tetrahydro-1-D-ribityl-1H-pyrazolo[3,4-d]pyrimidin-3-yl]butyl 1-Phosphate (14). Compound **30** (35.0 mg, 0.0480 mmol), methanol (0.75 mL), and concd HCl (0.5 mL) were added to a flask. The reaction mixture was stirred under reflux for 4.5 h. The solvent was removed under reduced pressure. Water (4 mL) was added, and the solution was filtered and frozen. The water was removed by freeze drying to generate the product (7.8 mg, 37.0%) as an amorphous white solid: 1H NMR (300 MHz, D_2O) δ 4.13–3.55 (m, 9H), 2.62–2.60 (m, 2H), 1.61–1.52 (m, 4H); ^{13}C NMR (75 MHz, D_2O) δ 161.1, 152.8, 152.5, 146.3, 97.8, 72.9, 72.3, 70.5, 66.6 ($^2J_{PC} = 5.6$ Hz), 62.8, 50.7, 29.4, 29.3, 26.7, 24.3; ESIMS m/z 763 (MNa^+); ESIMS m/z 439 (MH^+). Anal. Calcd for $C_{14}H_{23}N_4O_{10}P \cdot 4.5H_2O$: C, 35.77; H, 5.68; N, 11.92. Found: C, 35.89; H, 5.33; N, 11.36.

5-[4,6-Dioxo-4,5,6,7-tetrahydro-1-D-ribityl-1H-pyrazolo[3,4-d]pyrimidin-3-yl]pentyl 1-Phosphate (15). Compound **31** (59.2 mg, 0.080 mmol), methanol (1.25 mL), and concd HCl (0.83 mL) were added to a flask. The reaction mixture was stirred under reflux for 5 h. The solvent was removed under reduced pressure. Water (4 mL) was added, and the solution was filtered and frozen. The water was removed by freeze drying to generate the product (9.30 mg, 25.7%) as an amorphous white solid: 1H NMR (300 MHz, D_2O) δ 4.13–3.52 (m, 9H), 2.61–2.59 (t, $J = 5$ Hz, 2H), 1.52–1.22 (m, 6H); ^{13}C NMR (75 MHz, D_2O) δ 160.9, 152.7, 146.2, 97.6, 72.9, 72.2, 70.5, 67.0, 66.9 ($^2J_{PC} = 5.6$ Hz), 62.8, 50.6, 29.6, 29.5, 27.6, 26.9, 24.5; ESIMS m/z 475 (MNa^+). Anal. Calcd for $C_{15}H_{25}N_4O_{10}P \cdot H_2O$: C, 38.30; H, 5.79; N, 11.91. Found: C, 38.72; H, 5.58; N, 11.58.

Ethyl 3-[Bis(benzyloxy)phosphoryloxy]propanoate (19). Ethyl 4-bromobutyrate (1.17 g, 6.00 mmol) and the silver salt of dibenzyl phosphate (2.31 g, 6.00 mmol) were heated at reflux in dry toluene (50 mL) for 36 h under an atmosphere of argon. The solvent was filtered and evaporated to afford an oil. The oil was purified by silica gel flash chromatography, eluting with 3:2/2:1/2:1.5 hexane/ethyl acetate to afford the product (1.71 g, 72.8%) as a clean oil: 1H NMR (300 MHz, $CDCl_3$) δ 7.57–7.42 (m, 10H), 5.24–5.12 (dd, $^3J_{PH} = 8$ Hz, $^2J_{HH} = 12$ Hz, 4H), 4.29–4.22 (q, $J = 7$ Hz, 2H), 4.21–4.14 (dt, $^3J_{HH} = 6$ Hz, $^3J_{PH} = 6$ Hz, 2H), 2.51–2.46 (t, $J = 3$ Hz, 2H), 2.11–2.04 (p, $J = 7$ Hz, 2H), 1.43–1.37 (t, $J = 7$ Hz, 3H); ^{13}C NMR (75 MHz, $CDCl_3$) δ 172.5, 135.7 (d, $^3J_{PC} = 6.7$ Hz), 128.4, 127.8, 69.1 (d, $^2J_{PC} = 5.6$ Hz), 66.6 (d, $^2J_{PC} = 5.9$ Hz), 60.3, 30.0, 25.3 (d, $^3J_{PC} = 7.4$ Hz), 14.0; ESIMS m/z 415 (MNa^+). Anal. Calcd for $C_{20}H_{25}O_8P$: C, 61.22; H, 6.42. Found: C, 61.22; H, 6.41.²⁵

Ethyl 4-[Bis(benzyloxy)phosphoryloxy]butanoate (20). Ethyl 5-bromovalerate (2.59 g, 12.4 mmol) and the silver salt of dibenzyl phosphate (4.78 g, 12.4 mmol) were heated at reflux in dry toluene (98 mL) for 24 h under an atmosphere of argon. The solvent was filtered and evaporated to afford an oil. The oil was purified by silica gel flash chromatography eluting with 1:2/1:1 ethyl acetate/hexane to yield the product as a clean oil (2.97 g, 60%): 1H NMR (300 MHz, $CDCl_3$) δ 7.33–7.30 (m, 10H), 5.07–4.98 (dd, $^3J_{PH} = 8$ Hz, $^2J_{HH} = 12$ Hz, 4H), 4.13–4.06 (q, $J = 7$ Hz, 2H), 4.00–3.93 (dt, $^3J_{HH} = 6$ Hz, $^3J_{PH} = 6$ Hz, 2H), 2.27–2.23 (t, $J = 7$ Hz, 2H), 1.63–1.60 (m, 4H), 1.25–2.0 (t, $J = 7$ Hz, 3H).²⁵

Ethyl 5-[Bis(benzyloxy)phosphoryloxy]pentanoate (21). 6-Bromohexanoic acid ethyl ester (4.01 g, 18.0 mmol) and the silver salt of dibenzyl phosphate (6.93 g, 18.0 mmol) were heated at reflux in dry toluene (100 mL) for 24 h under an atmosphere of argon. The solvent was removed to provide a residue. The residue was purified by silica gel flash chromatography, eluting with 1:2/1:1 ethyl acetate/hexane to provide the product (5.78 g, 79.2%) as a clean oil: 1H NMR (300 MHz, $CDCl_3$) δ 7.53–7.49 (m, 10H), 5.18–5.17 (dd, $^3J_{PH} = 8$ Hz, $^2J_{HH} = 12$ Hz, 4H), 4.30–4.23 (q, J

$= 7$ Hz, 2H), 4.16–4.10 (dt, $^3J_{HH} = 6$ Hz, $^3J_{PH} = 6$ Hz, 2H), 2.43–2.39 (t, $J = 7.5$ Hz, 2H), 1.79–1.49 (m, 6H), 1.42–1.37 (t, $J = 7$ Hz, 3H); ^{13}C NMR (75 MHz, $CDCl_3$) δ 173.9, 136.3 (d, $^3J_{PC} = 6.8$ Hz), 129.0, 128.3, 69.6 (d, $^2J_{PC} = 5.6$ Hz), 68.0 (d, $^2J_{PC} = 6$ Hz), 60.7, 34.5, 30.3 (d, $^3J_{PC} = 7$ Hz), 25.4, 24.8, 14.7; ESIMS m/z 457 (MNa^+). Anal. Calcd for $C_{22}H_{29}O_8P$: C, 62.85; H, 6.95. Found: C, 62.57; H, 7.21.

4-(6-Chloro-2,4-dimethoxypyrimidin-5-yl)-4-oxobutanyl 1-Di-benzylphosphate (22). Dry THF (45 mL) was stirred and cooled to -30 °C under argon. *n*-BuLi (2.66 mL, 4.25 mmol) was added into the cooled THF, and the mixture was warmed to -10 °C for 30 min. The solution was cooled to -30 °C, and a solution of 4-chloro-2,6-dimethoxypyrimidine (0.74 g, 4.25 mmol) in THF (5 mL) was added. The reaction mixture was stirred at -30 °C for another 1.5 h. The mixture was cooled to -78 °C, compound **19** (1.67 g, 4.25 mmol) was added, and stirring was continued for 1 h at -78 °C. Hydrolysis was carried out at -70 °C using a mixture of 35% HCl (2 mL) and THF (10 mL). The reaction mixture was gently warmed to room temperature and made slightly basic with saturated sodium bicarbonate solution. The organic layer was separated. The aqueous layer was extracted with CH_2Cl_2 (3×10 mL). The extract was combined with the organic layer and dried with Na_2SO_4 overnight. The solvent was removed to provide a crude product, which was purified by silica gel flash chromatography, eluting with hexane/ethyl acetate 1.5:1/1:1 to generate the product (0.53 g, 31%) as a clear oil: 1H NMR (300 MHz, $CDCl_3$) δ 7.51–7.46 (m, 10H), 5.27–5.16 (dd, $^3J_{PH} = 8$ Hz, $^2J_{HH} = 12$ Hz, 4H), 4.30–4.22 (dt, $^3J_{HH} = 6$ Hz, $^3J_{PH} = 6$ Hz, 2H), 4.14 (s, 3H), 4.14 (s, 3H) 3.02–2.98 (t, $J = 7$ Hz, 2H), 2.22–2.18 (p, $J = 6$ Hz, 2H); ^{13}C NMR (75 MHz, $CDCl_3$) δ 119.4, 169.2, 164.3, 157.8, 136.2 (d, $^3J_{PC} = 6.8$ Hz), 129.0, 128.4, 115.0, 69.7 (d, $^2J_{PC} = 5.5$ Hz), 67.2 (d, $^2J_{PC} = 6$ Hz), 56.1, 55.6, 40.2, 24.6 (d, $^3J_{PC} = 7.5$ Hz); ESIMS m/z 543 (MNa^+). Anal. Calcd for $C_{24}H_{26}ClN_2O_7P$: C, 55.34; H, 5.03; N, 5.38. Found: C, 55.47; H, 5.10; N, 5.27.

5-(6-Chloro-2,4-dimethoxypyrimidin-5-yl)-5-oxopentanyl 1-Di-benzylphosphate (23). Dry 4-chloro-2,6-dimethoxypyrimidine (0.744 g, 4.26 mmol) was dissolved in dry THF (14 mL) under argon. The reaction mixture was cooled to -78 °C for 15 min, and a 1.6 M solution of *n*-BuLi in hexane (2.69 mL, 4.30 mmol) was added dropwise while maintaining the temperature below -70 °C. After stirring at -78 °C for 20 min, compound **20** (1.73 g, 4.26 mmol) in dry THF (4.5 mL) was added quickly, and the reaction mixture was allowed to slowly warm to -40 °C and stirred at -40 °C for 1 h. Brine (15 mL) was then added. The entire solution was extracted with ethyl acetate (30 mL) and dried with Na_2SO_4 overnight. After concentrating, the oil was purified by silica gel flash column chromatography, eluting with hexane/ethyl acetate 2:1/1:1 to afford the product (0.582 g, 25.6%) as a clean oil: 1H NMR (300 MHz, $CDCl_3$) δ 7.34–7.31 (m, 10H), 5.05–5.00 (dd, $^3J_{PH} = 8$ Hz, $^2J_{HH} = 12$ Hz, 4H), 4.01–3.96 (dt, $^3J_{HH} = 6$ Hz, $^3J_{PH} = 6$ Hz, 2H), 4.0 (s, 3H), 3.97 (s, 3H), 2.77–2.72 (t, $J = 6$ Hz, 2H), 1.71–1.68 (m, 4H); ^{13}C NMR (75 MHz, $CDCl_3$) δ 199.5, 168.7, 163.7, 157.2, 135.8 (d, $^3J_{PC} = 6.8$ Hz), 128.4, 127.8, 114.6, 69.1 (d, $^2J_{PC} = 5.5$ Hz), 67.3 (d, $^2J_{PC} = 6$ Hz), 55.5, 55.0, 43.0, 29.2 (d, $^3J_{PC} = 7.5$ Hz), 19.3; ESIMS m/z 535 (MH^+). Anal. Calcd for $C_{25}H_{28}ClN_2O_7P$: C, 56.13; H, 5.28; N, 5.24. Found: C, 55.75; H, 5.06; N, 5.16.

6-(6-Chloro-2,4-dimethoxypyrimidin-5-yl)-6-oxohexanyl 1-Di-benzylphosphate (24). Dry 4-chloro-2,6-dimethoxypyrimidine (0.748 g, 4.29 mmol) was dissolved in dry THF (12 mL) under argon. The reaction mixture was cooled to -78 °C for 10 min, and a 1.6 M solution of *n*-BuLi in hexane (2.90 mL, 4.64 mmol) was added dropwise while maintaining the temperature below -70 °C. After stirring at -78 °C for 30 min, compound **21** (1.80 g, 4.29 mmol) in dry THF (2 mL) was added quickly, and the reaction mixture was allowed to slowly warm to -40 °C and stirred at -40 °C for 1.5 h. The reaction mixture was slowly warmed to room temperature and stirred for 0.5 h. Brine (15 mL) was then added. The entire solution was extracted with ethyl acetate (35 mL)

and dried with Na_2SO_4 overnight. The organic solution was filtered, and the solvent was removed under reduced pressure to generate an oil. The oil was purified with silica gel flash chromatography, eluting with hexane/ethyl acetate 3:1/2:1 to afford the product (0.605 g, 26%) as a clean oil: ^1H NMR (300 MHz, CDCl_3) δ 7.55–7.54 (m, 10H), 5.29–5.22 (dd, $^3J_{\text{PH}} = 8$ Hz, $^2J_{\text{HH}} = 12$ Hz, 4H), 4.22 (s, 3H), 4.19–4.15 (dt, $^3J_{\text{HH}} = 6$ Hz, $^3J_{\text{PH}} = 6$ Hz, 2H), 4.17 (s, 3H), 2.97–2.92 (t, $J = 7$ Hz, 2H), 1.91–1.55 (m, 6H); ^{13}C NMR (75 MHz, CDCl_3) δ 201.6, 137.2 (d, $^3J_{\text{PC}} = 6.7$ Hz), 129.8, 129.1, 70.1 (d, $^2J_{\text{PC}} = 5.7$ Hz), 68.5 (d, $^2J_{\text{PC}} = 6.3$ Hz), 56.4, 55.9, 44.5, 30.5 (d, $^3J_{\text{PC}} = 7.5$ Hz), 25.4, 23.5; ESIMS m/z 571 (MNa^+). Anal. Calcd for $\text{C}_{26}\text{H}_{30}\text{ClN}_2\text{O}_7\text{P}$: C, 56.89; H, 5.51; N, 5.10. Found: C, 57.27; H, 5.50; N, 4.77.

3-(4,6-Dimethoxy-1H-pyrazolo[3,4-d]pyrimidin-3-yl)propyl 1-Dibenzylphosphate (25). Compound **22** (0.386 g, 0.742 mmol) and hydrazine (0.028 mL, 0.891 mmol) were added to methanol (65 mL). The mixture was kept at reflux under argon for 6 h. The solvent was removed in vacuo to give a residue. The residue was purified by column chromatography with hexane/ethyl acetate 1:1/1:1.5 as eluent to give pure product **25** (0.207 g, 56%) as a clear oil: ^1H NMR (300 MHz, CDCl_3) δ 7.14–7.08 (m, 10H), 4.92–4.81 (dd, $^3J_{\text{PH}} = 8$ Hz, $^2J_{\text{HH}} = 12$ Hz, 4H), 3.98–3.91 (dt, $^3J_{\text{HH}} = 6$ Hz, $^3J_{\text{PH}} = 6$ Hz, 2H), 3.89 (s, 3H), 3.87 (s, 3H), 2.85–2.80 (t, $J = 7$ Hz, 2H), 2.01–1.92 (p, $J = 6$ Hz, 2H); ^{13}C NMR (75 MHz, CDCl_3) δ 166.1, 165.0, 159.1, 146.2, 136.3 (d, $^3J_{\text{PC}} = 6.8$ Hz), 128.9, 128.3, 97.9, 69.7 (d, $^2J_{\text{PC}} = 5.6$ Hz), 67.8 (d, $^2J_{\text{PC}} = 6.2$ Hz), 55.6, 54.7, 29.4 (d, $^3J_{\text{PC}} = 7.2$ Hz), 25.0; ESIMS m/z 499 (MH^+). Anal. Calcd for $\text{C}_{24}\text{H}_{27}\text{N}_4\text{O}_6\text{P}$: C, 57.83; H, 5.46; N, 11.24. Found: C, 57.82; H, 5.31; N, 11.25.

4-(4,6-Dimethoxy-1H-pyrazolo[3,4-d]pyrimidin-3-yl)butyl 1-Dibenzylphosphate (26). Compound **23** (0.582 g, 1.09 mmol), methanol (25 mL), and hydrazine (41.8 mg, 1.31 mmol) were added to a flask. The mixture was stirred under reflux for 18 h. The reaction mixture was cooled to room temperature, and the solvent was removed under reduced pressure. The oil was purified by silica gel flash chromatography, eluting with hexane/ethyl acetate 1:4 to afford pure product (324 mg, 58.1%) as an oil: ^1H NMR (300 MHz, CDCl_3) δ 7.35–7.29 (m, 10H), 5.07–5.03 (dd, $^3J_{\text{PH}} = 8$ Hz, $^2J_{\text{HH}} = 12$ Hz, 4H), 4.11 (s, 3H), 4.09 (s, 3H), 4.07–4.03 (dt, $^3J_{\text{HH}} = 6$ Hz, $^3J_{\text{PH}} = 6$ Hz, 2H), 2.96–2.91 (t, $J = 7$ Hz, 2H), 1.83–1.70 (m, 4H); ^{13}C NMR (75 MHz, CDCl_3) δ 166.2, 165.1, 159.1, 147.2, 136.3 (d, $^3J_{\text{PC}} = 6.8$ Hz), 128.9, 128.3, 97.9, 69.6 (d, $^2J_{\text{PC}} = 5.6$ Hz), 68.1 (d, $^2J_{\text{PC}} = 6.1$ Hz), 55.6, 54.7, 30.1 (d, $^3J_{\text{PC}} = 7$ Hz), 28.3, 25.0; ESIMS m/z 513 (MH^+). Anal. Calcd for $\text{C}_{25}\text{H}_{29}\text{N}_4\text{O}_6\text{P}$: C, 58.59; H, 5.70; N, 10.93. Found: C, 58.52; H, 5.56; N, 10.78.

5-(4,6-Dimethoxy-1H-pyrazolo[3,4-b]pyrimidin-3-yl)pentyl 1-Dibenzylphosphate (27). Compound **24** (0.482 g, 0.880 mmol), methanol (20 mL), and hydrazine (56.32 mg, 1.76 mmol) were added to a flask. The mixture was stirred under reflux for 4 h, and then kept stirring at 45 °C for 12 h. The reaction mixture was cooled to room temperature. The solvent was removed under reduced pressure to afford an oil. The oil was purified by silica gel flash column chromatography, eluting with hexane/ethyl acetate 1:1/1:2 to yield the product (284.6 mg, 61.5%) as a clean oil: ^1H NMR (300 MHz, CDCl_3) δ 7.37–7.30 (m, 10H), 5.08–5.03 (dd, $^3J_{\text{PH}} = 8$ Hz, $^2J_{\text{HH}} = 12$ Hz, 4H), 4.18–4.12 (dt, $^3J_{\text{HH}} = 6$ Hz, $^3J_{\text{PH}} = 6$ Hz, 2H), 4.14 (s, 3H), 4.10 (s, 3H), 2.95–2.90 (t, $J = 7$ Hz, 2H), 1.81–1.44 (m, 6H); ^{13}C NMR (75 MHz, CDCl_3) δ 167.3, 166.1, 160.1, 148.6, 137.2 (d, $^3J_{\text{PC}} = 6.8$ Hz), 129.7, 129.1, 98.5, 70.0 (d, $^2J_{\text{PC}} = 5.6$ Hz), 68.6 (d, $^2J_{\text{PC}} = 6.1$ Hz), 55.9, 55.0, 30.5 (d, $^3J_{\text{PC}} = 7.1$ Hz), 28.9, 28.7, 25.6; ESIMS m/z 527 (MH^+). Anal. Calcd for $\text{C}_{26}\text{H}_{31}\text{N}_4\text{O}_6\text{P}$: C, 59.31; H, 5.93; N, 10.64. Found: C, 59.29; H, 5.80; N, 10.39.

3-[4,6-Dimethoxy-1-(2,2,6,6-tetramethyltetrahydro[1,3]dioxolo[4,5-e][1,3]dioxepin-4-ylmethyl)-1H-pyrazolo[3,4-d]pyrimidin-3-yl]propyl 1-Dibenzylphosphate (29). The protected ribityl iodide **28** (100 mg, 0.29 mmol) was added to the substituted pyrazolo[3,4-d]pyrimidine **25** (118 mg, 0.24 mmol) in DMF (3 mL). K_2CO_3 (98 mg, 0.15 mmol) was added to the reaction mixture. The reaction

mixture was stirred at room temperature for 3 days. The solvent was removed under reduced pressure. The residue was purified by silica gel TLC with hexane/ethyl acetate 1:3 as the mobile phase to afford product **29** (95 mg, 56%) as a clean oil: ^1H NMR (300 MHz, CDCl_3) δ 7.40–7.34 (m, 10H), 5.04–5.01 (dd, $^3J_{\text{PH}} = 8$ Hz, $^2J_{\text{HH}} = 12$ Hz, 4H), 4.57–4.54 (dd, $J = 4$, 9 Hz, 1H), 4.24–4.21 (m, 2H), 4.13–4.00 (m, 9H), 3.99–3.85 (m, 3H), 2.94–2.89 (t, $J = 7$ Hz, 2H), 2.08–2.03 (p, $J = 7$ Hz, 2H), 1.37 (s, 3H), 1.24 (s, 3H), 1.16 (s, 3H), 0.54 (s, 3H); ^{13}C NMR (75 MHz, CDCl_3) δ 165.9, 164.7, 157.9, 144.9, 136.3 (d, $^3J_{\text{PC}} = 6.8$ Hz), 128.9, 128.3, 109.2, 102.2, 98.1, 78.0, 69.6 (d, $^2J_{\text{PC}} = 5.5$ Hz), 69.3, 67.8 (d, $^2J_{\text{PC}} = 6$ Hz), 58.7, 55.4, 54.5, 49.1, 29.8 (d, $^3J_{\text{PC}} = 7.5$ Hz), 28.9, 26.3, 25.0, 24.3, 23.9; ESIMS m/z 713 (MH^+). Anal. Calcd for $\text{C}_{35}\text{H}_{45}\text{N}_4\text{O}_{10}\text{P}$: C, 58.98; H, 6.36; N, 7.86. Found: C, 59.09; H, 6.45; N, 7.70.

4-[4,6-Dimethoxy-1-(2,2,6,6-tetramethyl-tetrahydro[1,3]dioxolo[4,5-e][1,3]dioxepin-4-yl)-1H-pyrazolo[3,4-d]pyrimidin-3-yl]butyl 1-Dibenzylphosphate (30). Compound **26** (54.8 mg, 0.107 mmol), compound **28** (37.0 mg, 0.107 mmol), and potassium carbonate (44.3 mg, 0.321 mmol) were added into a flask. DMF (anhydrous, 2 mL) was added to the flask, and the reaction mixture was stirred under nitrogen at room temperature for 38 h. CHCl_3 (10 mL) was added, and the reaction mixture was filtered, washed with brine (8 mL), and then dried over Na_2SO_4 for 4 h. The solvent was removed under reduced pressure to yield the crude product (99 mg). It was purified by TLC with hexane/ethyl acetate 1:3 as the mobile phase to afford the product (35.0 mg, 45.1%) as an oil: ^1H NMR (300 MHz, CDCl_3) δ 7.14 (m, 10H), 4.84–4.82 (dd, $^3J_{\text{PH}} = 8$ Hz, $^2J_{\text{HH}} = 12$ Hz, 4H), 4.42–4.38 (dd, $J = 4$, 9 Hz, 1H), 4.07–3.71 (m, 14H), 2.69–2.64 (t, $J = 7$ Hz, 2H), 1.57–1.51 (m, 4H), 1.44 (s, 3H), 1.19 (s, 3H), 0.98 (s, 3H), 0.37 (s, 3H); ^{13}C NMR (75 MHz, CDCl_3) δ 165.9, 164.7, 157.9, 145.7, 136.3 (d, $^3J_{\text{PC}} = 6.8$ Hz), 129.0, 128.9, 128.3, 109.2, 102.2, 98.1, 78.1, 69.6 (d, $^2J_{\text{PC}} = 5.6$ Hz), 69.3, 68.0 (d, $^2J_{\text{PC}} = 6$ Hz), 58.7, 55.3, 54.5, 49.2, 30.1, 30.0 (d, $^3J_{\text{PC}} = 7$ Hz), 28.2, 26.3, 25.3, 24.3, 24.0; ESIMS m/z 727 (MH^+).

5-[4,6-Dimethoxy-1-(2,2,6,6-tetramethyl-tetrahydro[1,3]dioxolo[4,5-e][1,3]dioxepin-4-ylmethyl)-1H-pyrazolo[3,4-d]pyrimidin-3-yl]pentyl 1-Dibenzylphosphate (31). Compound **27** (100 mg, 0.190 mmol), **28** (65.4 mg, 0.190 mmol), and potassium carbonate (78.7 mg, 0.570 mmol) were added to a flask. Anhydrous DMF (2.5 mL) was added to the flask, and the reaction mixture was stirred under nitrogen for 3 days. CH_2Cl_2 (10 mL) was added, and the reaction mixture was filtered and washed with brine (5 mL). The aqueous phase was extracted with CH_2Cl_2 (3 \times 5 mL). The organic phases were combined and dried over Na_2SO_4 for 4 h. The solvent was removed under reduced pressure to generate an oil. The oil was purified by silica gel flash chromatography, eluting with hexane/ethyl acetate 1:1/1.5:1 to afford the product (63.0 mg, 44.8%) as a clean oil: ^1H NMR (300 MHz, CDCl_3) δ 7.30–7.24 (m, 10H), 5.01–4.97 (dd, $^3J_{\text{PH}} = 8$ Hz, $^2J_{\text{HH}} = 12$ Hz, 4H), 4.56–4.53 (dd, $J = 4$, 9 Hz, 1H), 4.23–3.85 (m, 14H), 2.82–2.77 (t, $J = 7$ Hz, 2H), 1.69–1.34 (m, 12H), 1.14 (s, 3H), 0.52 (s, 3H); ^{13}C NMR (75 MHz, CDCl_3) δ 165.9, 164.6, 157.8, 146.1, 136.4 (d, $^3J_{\text{PC}} = 6.8$ Hz), 128.9, 128.8, 128.3, 109.2, 102.2, 98.1, 78.0, 69.6 (d, $^2J_{\text{PC}} = 5.6$ Hz), 69.3, 68.2 (d, $^2J_{\text{PC}} = 6.1$ Hz), 58.7, 55.3, 54.5, 49.1, 30.3 (d, $^3J_{\text{PC}} = 7.1$ Hz), 29.0, 28.9, 28.6, 26.3, 25.5, 24.3, 23.9; ESIMS m/z 763 (MNa^+). Anal. Calcd for $\text{C}_{37}\text{H}_{49}\text{N}_4\text{O}_{10}\text{P}$: C, 59.99; H, 6.67; N, 7.56. Found: C, 59.61; H, 6.69; N, 7.39.

Kinetic Assays. All assays have been performed in 96-well microtiter plates using a computer-controlled SpectraMax 2 microplate reader (Molecular Devices GmbH, Ismaning, Germany). Enzymes used in kinetic assays are specified in the Table 3.

Lumazine Synthase Assay. Assay mixtures with variable concentrations of **1** contained 50 mM Tris hydrochloride, pH 7.0, 100 mM NaCl, 2% (v/v) DMSO, 5 mM dithiothreitol, 100 μM **2**, lumazine synthase, and **1** (3–150 μM) in a volume of 0.2 mL. Assay mixtures were prepared as follows. A solution (175 μL) containing 103 mM NaCl, 5.1 mM dithiothreitol, 114 μM **2**,

TABLE 3. Enzymes Used in Kinetic Assays

enzyme	organism	specific activity $\mu\text{M mg}^{-1} \text{h}^{-1}$	concn of enzyme in reaction mixture, $\mu\text{g mL}^{-1}$
lumazine synthases:	<i>B. subtilis</i>	8.7	2.0
	<i>S. pombe</i>	4.2	0.9
	<i>C. albicans</i>	4.4	1.5
	<i>M. grisea</i>	14.8	1.0
	<i>M. tuberculosis</i>	1.1	30
riboflavin synthases:	<i>E. coli</i>	20.6	1.1
	<i>M. tuberculosis</i>	4.1	4.0

and lumazine synthase in 51 mM Tris hydrochloride, pH 7.0, was added to 4 μL of inhibitor in 100% (v/v) DMSO (inhibitor concentration window, 0–300 μM) in a well of a 96-well microtiter plate. The reaction was started by adding 21 μL of a solution containing 103 mM NaCl, 5.1 mM dithiothreitol, and substrate **1** (30–1500 μM) in 51 mM Tris hydrochloride, pH 7.0. The formation of 6,7-dimethyl-8-ribityllumazine (**3**) was measured online for the period of 40 min at 27 °C at 408 nm ($\epsilon_{\text{lumazine}} = 10\,200 \text{ M}^{-1} \text{cm}^{-1}$).

For kinetic assays with variable concentrations of **2**, the concentration of **1** was set to 15 μM whereas the concentration of **2** in reaction mixture was varied between 30 and 400 μM . For kinetic assays in phosphate buffer, Tris hydrochloride and NaCl in reaction mixtures were replaced by 100 mM K/Na-phosphate pH 7.0. All other assay parameters were the same as described above.

Riboflavin Synthase Assay. Assay mixtures contained 50 mM Tris hydrochloride, pH 7.0, 100 mM NaCl, 1% (v/v) DMSO, 5 mM dithiothreitol, enzyme, and variable concentrations of **3** (3–50 μM) in a volume of 0.2 mL. Assay mixtures were prepared as follows. A solution (175 μL) containing 103 mM NaCl, 5.1 mM dithiothreitol, and riboflavin synthase in 51 mM Tris hydrochloride, pH 7.0, was added to 5 μL of inhibitor in 40% (v/v) DMSO (inhibitor concentration window, 0–400 μM) in a well of a 96-well microtiter plate. The reaction was started by adding 21 μL of a solution containing 103 mM NaCl, 5.1 mM dithiothreitol, and substrate **3** (30–500 μM) in 51 mM Tris hydrochloride, pH 7.0. The formation of riboflavin was measured online for the period of 40 min at 27 °C at 470 nm ($\epsilon_{\text{riboflavin}} = 9600 \text{ M}^{-1} \text{cm}^{-1}$).

Evaluation of Experimental Data. The velocity–substrate data were fitted for all inhibitor concentrations with a nonlinear

regression method using the program DynaFit.³⁰ Different inhibition models were considered for the calculation. K_i and K_{is} values \pm standard deviations were obtained from the fit under consideration of the most likely inhibition model as described earlier.²⁷

Lumazine Synthase Molecular Modeling. Using Sybyl (Tripos, Inc., version 7.1, 2005), the X-ray crystal structure of the complex of 3-(1,3,7-trihydro-9-D-ribityl-2,6,8-purinetrione-7-yl)butane 1-phosphate (**11**) and the lumazine synthase of *M. tuberculosis* (1w29) was downloaded and hydrogen atoms were added to the complex. The complex was first minimized using the steepest descent method to a termination gradient of 0.05 kcal/mol employing the MMFF94s force field and MMFF94 charges, and then the complex was minimized using the conjugate gradient method to a termination gradient of 0.05 kcal/mol. The structure of the inhibitor **14** was overlapped with the structure of 3-(1,3,7-trihydro-9-D-ribityl-2,6,8-purinetrione-7-yl)butane 1-phosphate (**11**), which was then deleted. The energy of the complex was first minimized using the steepest descent method to a termination gradient of 0.05 kcal/mol while employing the MMFF94s force field and MMFF94 charges, and then the complex was minimized using conjugate gradient method to a termination gradient of 0.05 kcal/mol. Figure 1 was constructed by displaying the amino acid residues of the enzyme that are involved in hydrogen bonding and stacking with the inhibitor **14**. The maximum distance between donor and acceptor atoms contributing to the hydrogen bonds shown in Figure 1 was set to 3.5 Å.

Acknowledgment. This research was made possible by NIH Grant GM51469, as well as by support from the Fonds der Chemischen Industrie and the Hans Fischer Gesellschaft. This investigation was conducted in a facility constructed with support from Research Facilities Improvement Program Grant Number C06-14499 from the National Center for Research Resources of the National Institutes of Health.

Supporting Information Available: ¹H and ¹³C NMR spectra of all new compounds, and Lineweaver–Burk plots for inhibition of lumazine synthases by inhibitor **14**. This material is available free of charge via the Internet at <http://pubs.acs.org>.

JO070982R

(30) Kuzmic, P. *Anal. Biochem.* **1996**, *237*, 260–273.